CONFERENCE PRE-PRINT

MACHINE ENHANCEMENT OF TOKAMAK DEVICE FOR THE JT-60SA NEXT OPERATION

H. Kayano
National Institutes for Quantum Science and Technology (QST)
Naka, Ibaraki 311-0193, Japan
Email: kayano.hiroki@qst.go.jp

A. Owada, A. Kaminaga, T. Nishiyama, T. Morimoto, K. Fukui, J. Yagyu and Y. Shibama

Abstract

The JT-60SA tokamak has entered the Maintenance & Enhancement phase 1 (M/E-1) from January 2024. In the M/E-1, JT-60SA is enhanced in order to allow high heating power operation with 3 MW ECRF and 23.5 MW NBI for deuterium plasma. Plasma facing components and its cooling system also be enhanced in accordance with the increased heat load from the main plasma. The paper reports the M/E-1 of tokamak devices such as enhancement in Vacuum Vessel (VV), water-cooling system for the in-vessels, and the improvement on the vacuum systems from the previous Integrated Commissioning (IC) in 2023. Measures taken on these issues are expected to contribute to robust plasma experimental operation, and to avoid reworks in the ITER commissioning beforehand.

1. INTRODUCTION

JT-60SA is the Superconducting (SC) tokamak device constructed under the framework of Broader Approach programme between Europe and Japan. Following the completion of the Operation Phase 1 (OP-1) [1], the JT-60SA tokamak, shown in Fig.1, has entered the M/E-1 in preparation for the Operation Phase 2 (OP-2). The main goals of the OP-2 include deuterium plasma operation, achieving plasma currents up to 5.5 MA, ITER risk mitigation and initial integrated scenarios development towards high confinement H-mode operation. A lower divertor with inertially cooled carbon tile is installed to allow a heat flux of 10 MW m^{-2} for 7.5 s and 15 MW m^{-2} for 5 s on the OP-2.

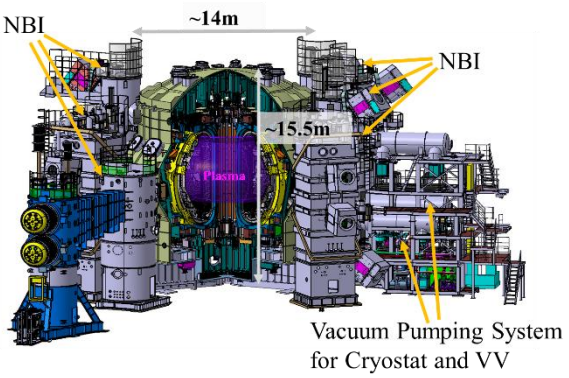

FIG. 1 Bird's eye view of the JT-60SA

During the M/E-1, JT-60SA is enhanced in order to allow high heating power operation with 3 MW ECRF and 23.5 MW Neutral Beam Injector (NBI) for deuterium. Plasma facing components and their cooling system are enhanced in accordance with the increased heat load from the main plasma. A minimum set of in-vessel components were installed for the OP-1 in order to product and control the plasma [2]. The remaining in-vessel components are installed during the M/E-1, as illustrated in Fig.2. In parallel with the these in-vessel works, insulation of the SC coil is reinforced in the Cryostat, because plasma operation with a maximum plasma current is a target in the OP-2, which requires all the SC coil systems to achieve their nominal coil current and voltage.

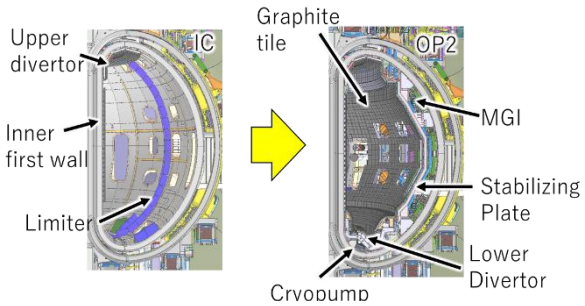

FIG. 2 Enhancement of the in-vessel component for the OP2

High heating power operation starts with the OP-2, and hydrogen operation is carried out to avoid excessive neutron generation and machine activation at the beginning. Thereafter, deuterium operation starts. There are many scientific topics in the OP-2 in the area of operation regime development [3]. Plasma current will be increased step by step.

To achieve the machine targets described above, the tokamak components must be enhanced to ensure compatibility with the heating systems and the in-vessel water-cooling system. Other improvements to the vacuum pumping system are (i) measures for the two Dry vacuum Pump (DRP) failures in cryostat vacuum pumping during the IC in 2023 and (ii) enhancement in the vacuum interlock (I/L) system to ensure safe termination of the SC system in the event of vacuum degradation. Details of issues and improvements of the JT-60SA device gained through these activities are of importance for ITER.

In the paper, installation of ports and water circulation system are reported in the section 2, improvements in vacuum system from the IC are reported in the section 3, and this report is summarized in the section 4.

2. PREPARATION FOR THE HIGH-POWER HEATING

The JT-60SA is designed for a maximum heating power of 41 MW, among the highest-class heating systems worldwide. To realize the high-power plasma heating, the VV is required to install additional ports for new equipment such as NBI and diagnostics. Plasma pulses of up to 100 s are planned. To remove the heat load on in-vessel components, due to high heat flux and long duration, the water cooling system needs to be enhanced. Installing these components requires high-precision alignment and ensuring electrically insulation of each component throughout assembly.

2.1. Additional Port Installation for High-power Plasma Heating Operation

At the time of the OP-1, there are 55 port penetrations out of 73 port bores to the inside the VV. Rest 18 ports penetration and 5 joints to connect NBI tank, shown in Fig.3, are scope of the M/E-1. Those ports are used for new equipment such as P-NBI, diagnostics and water piping. The NBI system used in the JT-60U are re-used in JT-60SA, the NBI tanks are reinstalled at the same locations as in the JT-60U. The JT-60U is tokamak device which uses normal conducting magnet, thus, it didn't equip cryostat. Spatial condition is much narrower in JT-60SA. Owing to clearance with NBI tanks, tolerance of the NBI port is ±2 mm at its centerline, and the other ports is ±5 mm.

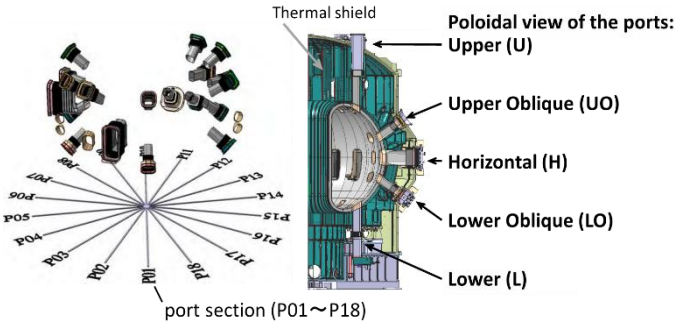

FIG. 3 Additional 18 port (left) and cross section of tokamak

Dimensions of the CV are approximately 15.5 m high and 14 m diameter, as shown in Fig.1, and the dimension of the VV are 6.6 m high and 10 m outer diameter. In accordance with the device's scale, the ports are large and heavy, this makes fine positioning by human-power impractical. To install the ports, dedicated hanging jig and fixing jig, aliment jig are applied. As for the welding, a small amount of welding distortion can lead deformation in these large-scale structures. Compared to the typical port length of 1.6 m, as illustrated in Fig. 4, installation tolerance of ±2 mm is severe and ensuring the tolerance is highly challenging. To achieve the high precision, port positions are measured using laser trackers and dial gauge as installation of the VV [4]. The port is composed of a port pipe, electrical insulation, and bellows designed to absorb displacements. To minimize on-site installation work at the narrow space, the port was combined as an integrated port. A joint to connect with NBI tank was installed for the NBI port.

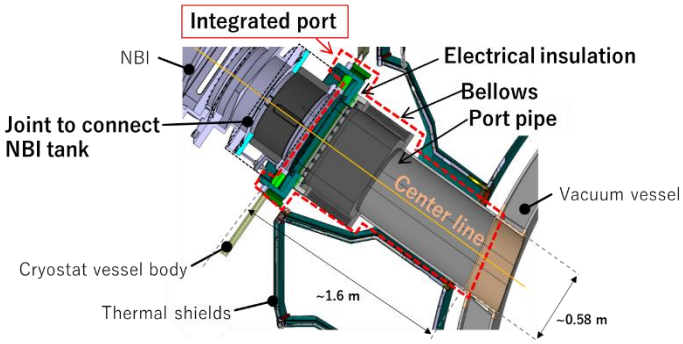

FIG. 4 Outline of integrated port of NBI

To ensure that induced currents flow only in the designed loop circuits during plasma operation, the VV is

electrically insulated from the CV which is ground potential. Because welding using high-current is performed in the VV, to prevent the occurrence of stray currents the electrical potential between VV and CV must be continuously separated throughout all installation procedures. Thus, insulating materials were incorporated into the fixing jigs, and installation procedures to maintain insulation were established.

FIG. 5 Port installation

All 18 ports that had been scheduled to be installed by the OP-2 are indicated in Fig. 3. By July 2025, installation of all ports was completed. In addition to 55 ports already installed, such as upper and lower vertical ports, installation of all 73 ports on the JT-60SA has finely completed as planned.

SC coil insulation reinforcement is another important activity for the OP-2 [5]. Following Equilibrium Field coil #1 (EF1) electrical short incident during the IC in 2021. Insulation reinforcement on SC coil terminal has already been carried out. However, there were still locations where reinforcement is needed but too narrow to access. Such locations need removal of nearby structures such as port and thermal shields. To prepare for SC coil repairments, duct materials on P01H, P11H, P14H, P11UO and P14UO were mill-machined, as described in Fig.6. After the SC coil repairments work, bores are being filled out by the same thickness plate.

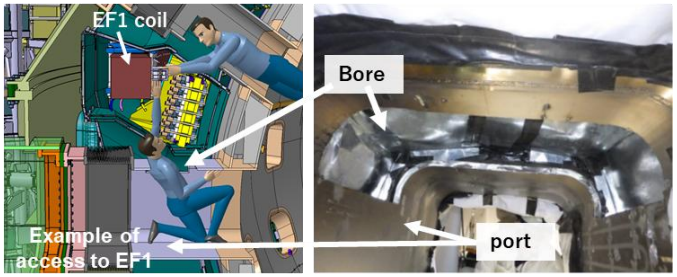

FIG. 6 Access simulation of EF coil insulation reinforcement (left) and bore mill-machined (right) on port pipe

2.2. Water Cooling System for Long-pulse Plasma

A water-cooling system is being introduced to remove heat flux in in-vessel components such as the lower divertor, first wall, NBI port protection plate, in-vessel coil. Table.1 shows the enhancement plan for the cooling water piping and circulation system. At integrated research phase, total heating power of 41 MW duration of 100 s is planned. As for heat removing capacity, a heat load of 50 MW duration of 100 s are set as design specification.

Table. 1 Enhancement plan of the cooling water piping and circulation system

Research phase	**Initial research phase**		**Integrated research phase**
OP	**OP-1**	**OP-2 ~ OP-4**	TBD
Piping	No	Enhanced	Used (partially improved)
Water circulation system	Not maintained	Re-use of JT-60U (~ 500m^3/h ,~1.4MPa at pump)	Enhanced to full specification (~3000m^3/h , >2MPa)

The water piping and the overall layout of the cooling water circulation system are shown in Fig. 7. During the initial research phase, the water circulation system in the JT-60U including pumps, heat exchangers, and ion-exchange towers are maintained and re-used. This approach contributes to shorten the preparation time and the early provision of cooling water for the OP-2 – OP-4. In the OP-2, high heat fluxes with durations on the order of seconds will be applied to in-vessel components, for example, 10 MW m^{-2} for 7.5 s and 15 MW m^{-2} for 5 s on the lower divertor are planned. In-vessel components heated by a plasma shot are inertially cooled during inter-shot interval (≈30 min) by cooling water supplied below 40 °C. The warmed water is collected in a tank and transfers heat to a secondary water circulation system via heat exchangers installed on the purification line and the main circulation line. The heat accumulated in the cooling water is removed during

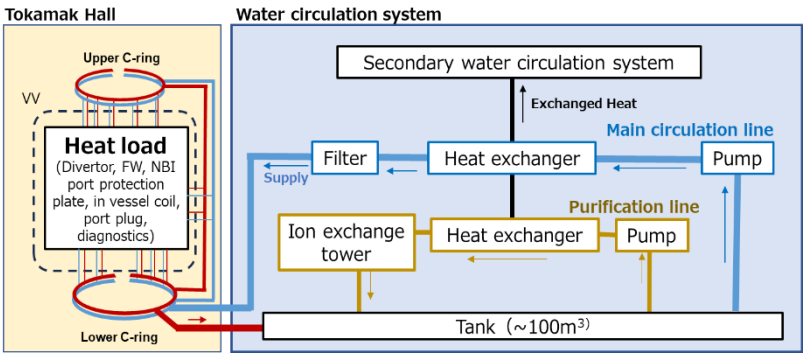

FIG. 7 schematic drawing of the water circulation system during the Initial Research Phase

overnight periods when no plasma shots are performed. Regarding water conductivity, the ion-exchange towers were used to remove copper ions originating from the copper-alloy on heatsinks such as divertor and first wall.

Regarding the piping layout in the tokamak hall, in order to supply cooling water from the nearest ports to in-vessel components installed at various locations around 360° (from P01 to P18), supply and return headers were designed in a C-shaped configuration (C-ring) surrounding both the upper and lower sections of the CV. Lower C-ring have been installed and upper C-ring is being installed. By installing C-ring headers close to the tokamak, the total length of individual piping is reduced, thereby lowering the risk of spatial interference in the confined space of the tokamak hall. Parts of as piping are already installed as shown in Fig. 8.

FIG. 8 Water piping installed under Tokamak-hall

The cooling water piping must pass several requirements; (i) to withstand the specified design pressure; (ii) to maintain electrical isolation between the VV potentials; and (iii) to be compatible with the operational demands of tokamak systems. A large number of cooling pipes are enhanced, as shown in piping of Fig. 9. The water lines were designed and manufactured with consideration of baking and long-term maintenance operational scenarios. Since it is necessary to fill and drain the water during baking operations and long-term maintenance, air-vent valves were installed. Corresponding drain piping and valves are installed at lower location of each water line. To regulate the flow rate according to the specified heat removal performance for each water line, a butterfly valve was adopted. A remote control will become necessary after an increase in radiation levels, valves capable of both manual and pneumatic operation were selected. Displacements during baking or seismic events are required to be absorbed. Expansion joints and expansion piping were used at each connection. Insulation is adopted to ensure each electrical isolation of the water piping, the VV and the CV.

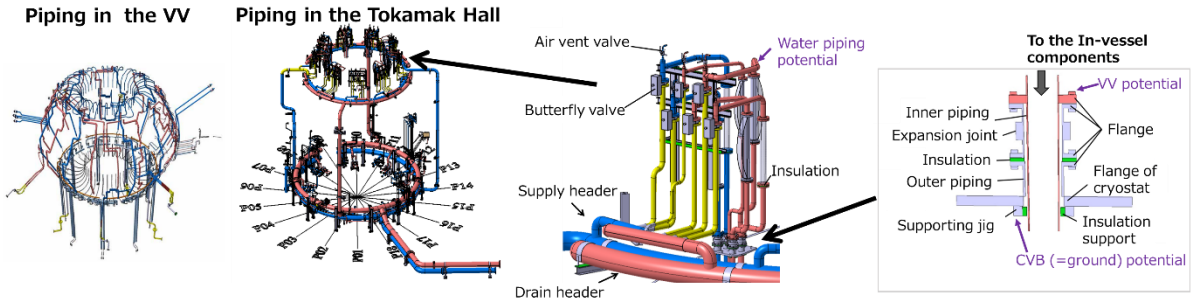

FIG. 9 Bird's eyes view and design of cooling water piping in the Tokamak-hall

With the installation of ports and the cooling-water circulation system, preparations for the next high-power plasma operation are progressing. In the M/E-1, in addition to these activities, improvements to the issues identified in the OP-1 are being performed for the robust tokamak operation in the OP-2 as reported section below.

3. IMPROVEMENTS IN VACUUM SYSTEM FROM INTEGRATED COMMISSIONING

During the SC energization test in March 2021, a sudden increase in the cryostat internal pressure was observed. A subsequent investigation identified that a short circuit at the EF1 terminal joints had caused a helium-coolant leak. Terminal joint of EF coil was damaged [6]. Following the repairment in the CV, the electrical insulation of the SC terminal were restored [7]. This section first reports on improvement in the cryostat vacuum pumping system following the repairment, and second reports on a protective I/L system to detect abnormal degradation of the cryostat vacuum.

3.1. Cryostat Vacuum Pump Failure and Measure

In the CV, vacuum pumping is carried out under more severe conditions than in the VV, owing to carbon compounds such as polyamide and polyester, and aluminium which constitute multi-layer insulation. The multi-layer insulation covers large parts of thermal shields and has large area shown in Fig.3. In addition to this carbon compound material, after the short circuit incident of the IC in 2021, the electrical insulation of the terminal joints

and of feeders with similar structures was reinforced with resin. Fig. 10 shows the CV pressure from the start of vacuum pumping in 2020 and in 2023. As an example, approximately 20 minutes after pumping started, the pressure had reached about 10^{-1} Pa in 2020, whereas it was about 10 Pa in 2023. Major difference on the CV vacuum between 2020 and 2023 is insulation reinforcement, thus this difference is attributed to the outgassing from material brought on insulation-repair work. The cryostat is exhausted with vacuum pumping system, as shown in Fig. 11. During the IC in 2023, two DRPs (out of five) used in the cryostat vacuum pumping system failed. In that case of the IC in 2023, the cryostat was exhausted using other fore-line pumps through the bypass line prepared in advance.

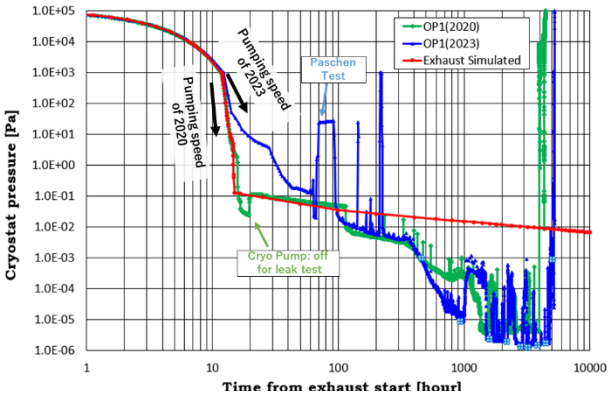

FIG. 10 Time dependence of the cryostat pressure in 2020 and 2023

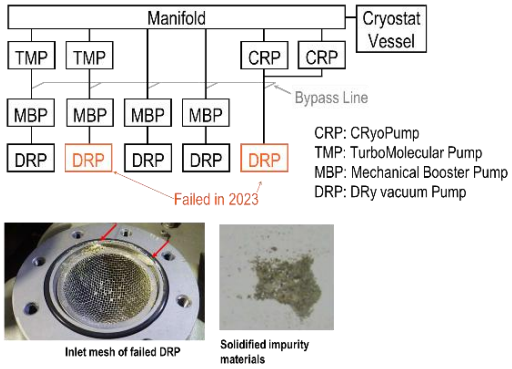

FIG. 11 Schematic diagram of the cryostat vacuum pumping (Upper) and impurities found at DRP (Lower)

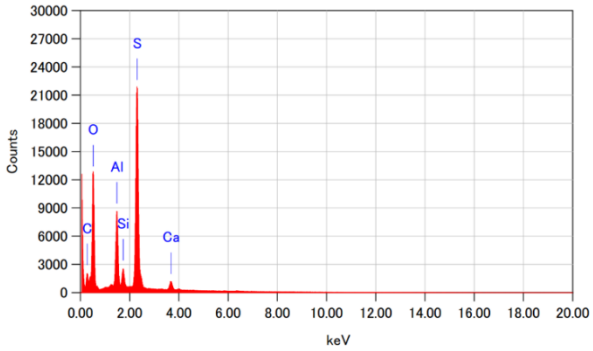

FIG. 12 Elemental analysis result of energy-dispersive X-ray spectroscopy (EDS)

By the subsequent visual investigation, solidified impurities were found at inlet mesh of DRP and damages of the pump bearings were confirmed. One of the causes of the failure is estimated to be damage to the bearings caused by impurities. Elemental analysis of solidified impurity was conducted to identify the cause, as shown in Fig. 12. Result of energy-dispersive X-ray spectroscopy suggest that the major elements are sulphur, aluminium, oxygen, carbon and silicon. These impurities are considered to originate from multilayer insulation materials and materials brought in during insulation repair, such as machining oil, and resin.

During compression in the pump, liquefaction or solidification occurs if the partial pressure of a condensable impurity exceeds its saturation pressure. Let x_{cond} denote mole fraction of the condensable gas at the pump inlet, a non-condensation condition for the compression zone is given below.

$$x_{cond} < \frac{p_{cond,sat}\,(T_{comp})}{P_{comp}}$$

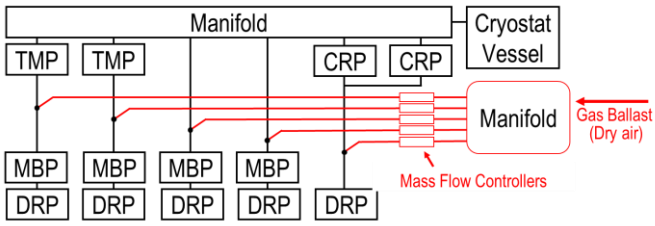

FIG. 13 Schematic drawing of gas ballast system

Where, P_{comp} and T_{comp} are total pressure and temperature in the compression zone of the pump, respectively. $p_{cond,sat}\,(T_{comp})$ is saturation pressure of the condensable gas. Mole fraction can be written as $x_{cond} = p_{cond,in}/P_{in}$, here $p_{cond,in}$ is defined as the partial pressure of the condensable gas at the pump inlet and P_{in} is defined as the total pressure at the same location.

To prevent condensation, a gas ballast system will be employed, as shown in Fig. 13. The gas ballast system will inject dry air (permanent gas) and decrease the mole ratio of condensable gas before compression. Regarding the

dilution ratio, we assume that gas arriving at ≤ 1 Pa will be diluted by at least ten times and then delivered to the downstream pumps. The actual dilution ratio will be adjusted during commissioning, taking into account cryostat vacuum level, result of mass analyser on-time, and degradation of the compression ratio of upstream TMP. In addition, other improvements will be implemented to address anticipated cause of pump failure, including modification to the water-drain, to ensure robust cryostat vacuum pumping during the OP-2.

3.2. Vacuum Interlock Gauges for Reliable Superconducting Coil Protection

An abnormal degradation of the CV vacuum during SC energization has been identified as a potential risk of discharges that could cause severe damage to the device [8,9]. The voltage occur electrical discharge is a function of pressure and the gap between terminals, according to Paschen's law. However, the presence of a magnetic field can lead to electrical discharge at either lower or higher voltages than predicted by Paschen's law. Furthermore, during operation, the magnetic field varies continuously, and the geometry in cryostat is highly complex. Based on the experience gained from previous insulation reinforcements and the global Paschen tests already conducted, it is considered difficult to ensure that the JT-60SA tokamak as "Paschen-proof". Instead of relying solely on insulation reinforcement, a defence-in-depth approach has been adopted by implementing multiple redundant measures, such as reducing the voltage requirements of the SC coil and monitoring the CV vacuum.

As measures for monitoring the cryostat vacuum, a coil protective I/L system, that rapidly detects abnormal vacuum degradation and achieve safely termination of SC coil, has been constructed from the OP-1 and improvements to increase system reliability are being implemented.

Several types of monitoring devices are employed on JT-60SA, including spark wires, helium leak detectors, Cold Cathode Gauges (CCG). There are two types of CCG; a self-product CCG and a commercial CCG. The self-product CCG is called C-CCG (Cryogenic CCG). Sensors of C-CCG operated in the range of 4 K to room temperature and installed near the magnets, where the operating environment is severe, to detect helium leakage as early as possible. Details of spark wires and C-CCG are described in [6,10]. Commercial CCG, called R-CCG (Room temperature CCG), installed on the CV focus on reliable operation owing to 1) designed for ITER and operating environment has been verified [11], 2) it is installed in a relatively low magnetic field environment with room temperature. This section focuses on the design and enhancement of the R-CCG.

3.2.1. Outline of vacuum gauge on port section 02

A R-CCG was installed at port section 2 of the bottom of the CV at the OP-1, called R-CCG on P02. As shown in Fig.14. Sensor head consists with a Pirani gauge and a CCG. Sensor head are separated from the measuring card which converts raw sensor-signal to the electrical signal. This makes it possible to place measuring cards away from the tokamak device. This contributes to increase measurement system's resistance to magnetism and radiation. Threshold to send vacuum degradation signals is set at 1×10^{-4} Pa considering vacuum in normal operation and noise signal.

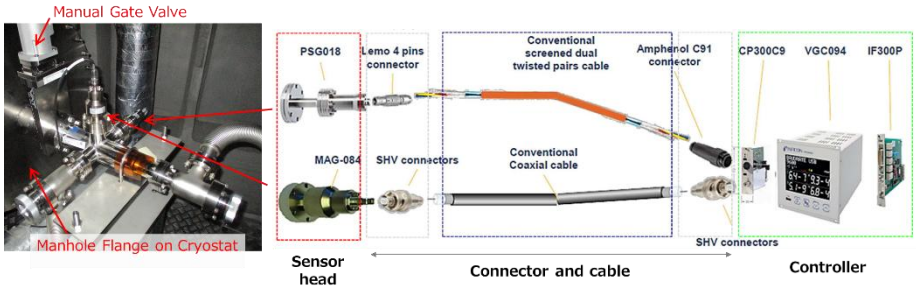

FIG. 14 Vacuum gauge using R-CCG for the Coil protection interlock system

3.2.2. *Test onsite in the OP-1*

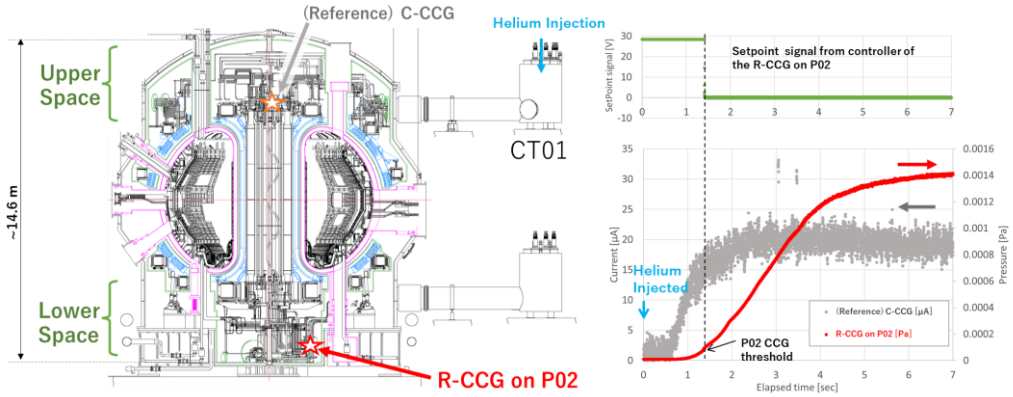

FIG. 15 Response of the R-CCG on P02 corresponding to the Helium injection from CT01

The I/L vacuum gauges were tested several times in actual equipment using helium gas of ~25 Pam^3 during the IC in 2023 [9]. Fig. 15 shows the cryostat geometry and the response of the R-CCG on P02 during an onsite test conducted in December 2023, when coil was cooled to cytogenetic temperature. After the helium gas injection, the helium spreads throughout the cryostat from upper space to lower space. The pressure at the R-CCG on P02 exceeded threshold (10^{-4} Pa) at 1.39 s after injection, and the controller of the CCG output setpoint signals at 1.41 s. As a reference, response of a C-CCG installed in the upper space of the cryostat was also described. Although it exhibits a higher noise level, it is confirmed that the C-CCG detect pressure increases on the order of a half a second earlier than the R-CCG on P02, located in the lower space of the cryostat.

3.2.3. *Enhancement of CCG for OP-2*

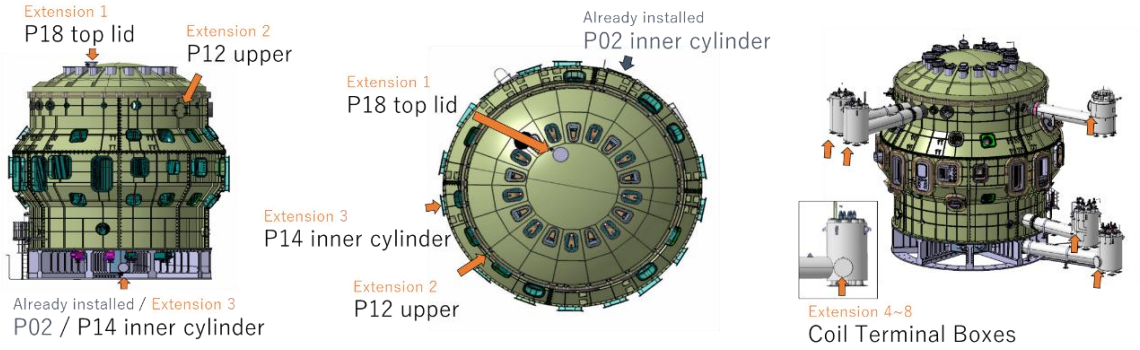

FIG. 16 Location of manholes which R-CCG will be enhanced in the M/E-1

To improve the overall detection response of R-CCG, additional CCGs will be installed at several locations on the CV during the OP-2. Additional three I/L vacuum gauges on the CV body and five on Coil Terminal Box (CTB) are planned to be enhanced, as shown in Fig. 16. This enhancement contributes to the fast response and increase system redundancy. The reduction in detection time depends on the assumed leak rate and the location of the leak in the complex cryostat structure and components. However, based on the onsite test results, a reduction on the order of a half a second can be expected.

As for the C-CCG, the 2nd generation C-CCG will be developed and installed to improve its detection performance for the OP-2 operation.

4. SUMMARY

Recent machine enhancements on the JT-60SA tokamak device to achieve high-temperature, high-density plasmas and enable robust operation in the next operation (OP-2) are reported.

- To enhance equipment necessary to achieve high performance plasma, such as NB system and diagnostics, 18 ports and 5 joints required to be installed. All port and joints have been installed. Including 55 ports which had already been installed, the installation of all 73 ports, specified in the device design, has been completed.
- To remove high heat loads from in-vessel components such as the first wall and lower divertor, cooling water piping is manufactured, and parts of piping is installed on the tokamak.
- During the IC in 2023, two dry vacuum pumps failed. One of the reasons is solidification of material pumped from the cryostat vacuum. To prevent DRPs from failure, gas ballast system, to suppress condensable partial pressures, is selected as measure and planned to be enhanced.
- To mitigate the risk of discharge accidents caused by gas leaks inside the CV, the number of R-CCG will be increased from one to eight. By this enhancement redundancy and response speed are improved.

These enhancements and corrective measures are expected to contribute to achieving the scope of the OP-2, generating high-temperature, high-density plasmas with a maximum plasma current of 5.5 MA. Measures taken on issues on the OP-1 are expected to contribute robust plasma experimental operation on JT-60SA next operation, and to avoid reworks in the ITER commissioning beforehand.

ACKNOWLEDGEMENTS

JT-60SA was jointly constructed and is jointly funded and exploited under the Broader Approach Agreement between Japan and EURATOM. The first author acknowledges the colleagues in the JT-60SA Tokamak Device Group for their supports and encouragements and the JT-60SA Magnet System Group for their sincere supports and fruitful discussion.

REFERENCES

[1] K. Takahashi, et al., Fusion Eng. Des. 216 (2025) 115059.
[2] M. Takechi, et al., Fusion Eng. Des. 168 (2021) 112572.
[3] JT-60SA Research Unit 2018 JT-60SA research plan (version 4.0) (available at: www.jt60sa.org/wp/wp-content/uploads/ 2021/02/JT-60SA_Res_Plan-5.pdf)
[4] Y. Shibama, et al., Fusion Eng. Des. 125 (2017) 1-8.
[5] K. Tsuchiya., et al., “Performance of JT-60SA Superconducting Magnet Operation in Integrated Commissioning Test”, Preprint:2025 IAEA Fusion Energy Conf. [ID: 2727]
[6] K. Hamada, et al., IEEE Trans. Appl. Supercond. 34 (2024) 4200805.
[7] H. Shirai, et al., Nucl. Fusion. 64 (2024) 112008.
[8] J. Knaster, et al., Trans. Appl. Supercond. 22 (2012) 9002904.
[9] K. Khumthong et al., Trans. Appl. Supercond. 34 (2024) 4205506.
[10] K. Fukui, et al., IEEE Trans. Appl. Supercond. 35 (2025) 4202005.
[11] INFICON, Datasheets of MAG084 Cold Cathode Gauge. [Online] Available: https://www.inficon.com/media/11155/download/MAG084-Cold-Cathode-Gauge.pdf